of human diabetic pancreatic β cells, it is not possible to assess directly the relative importance of the different cellular actions of the sulfonylureas on the hypoglycemic action of these compounds in vivo. Our data suggest that in a depolarized β cell, the direct effect of the sulfonylureas on exocytosis may account for as much as 75% of the total stimulatory action (*8*). This figure would represent the maximum contribution because in β cells that are not voltage-clamped, the sulfonylureas will also stimulate secretion by producing membrane depolarization, acceleration of Ca^{2+} influx, and enhancement of Ca^{2+}-dependent exocytosis (*15*). The effects of tolbutamide on exocytosis can be observed at concentrations only slightly higher than those required to block the K_{ATP} channels and that are within the therapeutic range (*16*). The potentiation of exocytosis we report here is therefore likely to contribute to the insulinotropic and hypoglycemic actions of the sulfonylureas in diabetic patients.

REFERENCES AND NOTES

1. F. M. Ashcroft and S. J. H. Ashcroft, in *Insulin: Molecular Biology to Pathology*, F. M. Ashcroft and S. J. H. Ashcroft, Eds. (IRL Press, Oxford, 1992), pp. 97–150.
2. W. Kramer, R. Oekonomopulos, J. Punter, H.-D. Summ, *FEBS Lett.* **229**, 355 (1988); L. Aguilar-Bryan, D. A. Nelson, Q. A. Vu, M. B. Humphrey, A. E. Boyd, *J. Biol. Chem.* **265**, 8214 (1990); H. Bernardi *et al.*, *Proc. Natl. Acad. Sci. U.S.A.* **90**, 1340 (1993).
3. L. Aguilar-Bryan *et al.*, *Science* **268**, 423 (1995); N. Inagaki *et al.*, *ibid.* **270**, 1166 (1995).
4. S. E. Ozanne, P. C. Guest, J. C. Hutton, C. N. Hales, *Diabetologia* **38**, 277 (1995); J. L. Carpentier, F. Sawano, M. Ravazzola, W. J. Malaisse, *ibid.* **29**, 259 (1986).
5. Whole-cell currents were elicited by depolarizations to 0 mV from individual tissue-cultured mouse β cells with the use of the perforated patch whole-cell configuration [M. Lindau and J. M. Fernandez, *Nature* **319**, 150 (1986); R. Horn and A. Marty, *J. Gen. Physiol.* **92**, 145 (1988)]. Exocytosis was monitored as changes in membrane capacitance [E. Neher and A. Marty, *Proc. Natl. Acad. Sci. U.S.A.* **79**, 6712 (1982); C. Joshi and J. Fernandez, *Biophys. J.* **53**, 885 (1988)]. Depolarizations were applied at 2-min intervals to avoid depression of the exocytotic responses. The extracellular medium consisted of 118 mM NaCl, 20 mM tetraethylammonium chloride, 5.6 mM KCl, 1.2 mM $MgCl_2$, 2.6 mM $CaCl_2$, and 5 mM Hepes (pH 7.4 with NaOH). Glucose was usually present at a concentration of 5 mM, but similar effects were observable in its absence. Forskolin, PMA, and most pharmacological agents were dissolved in dimethyl sulfoxide (DMSO; final concentration, 0.01 to 0.1%) and were included in the extracellular medium as indicated. It was ascertained that these concentrations of DMSO do not interfere with the exocytotic responses. The pipettes were filled with 76 mM Cs_2SO_4, 10 mM NaCl, 10 mM KCl, 1 mM $MgCl_2$, and 5 mM Hepes (pH 7.35 with CsOH). Electrical contact was established by insertion of the pore-forming antibiotic amphotericin B [J. Rae *et al.*, *J. Neurosci. Methods* **37**, 15 (1991)] (final concentration, 0.24 mg/ml) to the pipette solution. All electrophysiological experiments were done at 32° to 34°C. Data are presented as mean values ± SEM of the stated number of experiments, and statistical evidence was evaluated with the Student's *t* test for paired data with each cell serving as its own control.
6. An increase in capacitance can be equated to exocytosis (*17*) and is unlikely to result from charge movements that occur because of the gating of voltage-dependent (Na^+) channels [see F. T. Horrigan and R. J. Bookman, *Neuron* **13**, 1119 (1994)] because (i) inhibition of the voltage-gated Ca^{2+} channels with Co^{2+} abolishes depolarization-evoked capacitance changes [C. Ämmälä *et al.*, *J. Physiol. (London)* **474**, 665 (1993)] and (ii) lowering the temperature from +34°C to room temperature suppresses exocytosis (and capacitance increases) while not much affecting the properties of the voltage-gated currents (E. Renström, L. Eliasson, P. Rorsman, in preparation).
7. C. Ämmälä, F. M. Ashcroft, P. Rorsman, *Nature* **363**, 356 (1993).
8. In the simultaneous presence of both 17 mM glucose and 40 mM K^+, the sulfonylurea glibenclamide (2 μM) increased insulin secretion by 210 ± 70% (from 1.50 ± 0.19 ng per 20 islets per 10 min to 4.24 ± 0.87 ng per 20 islets per 10 min; $P < 0.01$ versus the value observed in the presence of glucose and K^+ alone). Experiments were performed at 37°C. Values are means ± SEM of nine experiments carried out on three preparations of islets.
9. D. Toullec *et al.*, *J. Biol. Chem.* **266**, 15771 (1991). At the concentration used (2.4 μM), the inhibitor suppressed the stimulatory effect of PMA but had no effect on exocytosis stimulated by forskolin.
10. C. Ämmälä *et al.*, *Proc. Natl. Acad. Sci. U.S.A.* **91**, 4343 (1994).
11. $[Ca^{2+}]_i$ was measured in parallel with the electrophysiological recordings by dual wavelength microfluorimetry as described (*17*) with the use of fura-2 as the indicator. Before the measurements, the cells were loaded with the ester form (0.1 μM) of fura for 20 min.
12. G. Trube, T. Ohno-Shosaku, P. Rorsman, *Pfluegers Arch.* **407**, 493 (1986); J. Zünkler *et al.*, *Naunyn-Schmiedeberg's Arch. Pharmacol.* **337**, 225 (1988).
13. F. Thévenod *et al.*, *J. Membr. Biol.* **129**, 253 (1992).
14. L. H. Philipson, *Science* **270**, 1159 (1995); C. F. Higgins, *Cell* **82**, 693 (1995).
15. Mouse diabetic β cells are permanently depolarized even at subthreshold glucose concentrations [H. P. Meissner and H. Schmidt, *FEBS Lett.* **67**, 37 (1976)].
16. U. Panten, M. Schwanstecher, C. Schwanstecher, *Horm. Metab. Res.* **24**, 549 (1992).
17. K. Bokvist *et al.*, *EMBO J.* **14**, 50 (1995).
18. The phase angle was determined for each experiment. The absence of a change in cell conductance associated with the depolarizations indicates that the phase angle was correctly set and that the observed step changes of membrane capacitance are not attributable to variations of cell conductance.
19. R. W. De Wit *et al.*, *Eur. J. Biochem.* **142**, 255 (1984).

20. L.E. and E.R. contributed equally to this study and their names appear in alphabetical order. Supported by the Juvenile Diabetes Foundation International, the Swedish Medical Research Council, the Nordic Insulin Foundation Committee, National Institutes of Health, and the Swedish Diabetes Association.

26 July 1995; accepted 8 December 1995

Cold-Induced Expression of Δ^9-Desaturase in Carp by Transcriptional and Posttranslational Mechanisms

P. E. Tiku, A. Y. Gracey, A. I. Macartney, R. J. Beynon, A. R. Cossins*

Poikilothermic animals respond to chronic cold by increasing phosphoglyceride unsaturation to restore the fluidity of cold-rigidified membranes. Despite the importance of this compensatory response, the enzymes involved have not been clearly identified, and the mechanisms that control their activity are unknown. In carp liver, cold induces an 8- to 10-fold increase in specific activity of the microsomal stearoyl coenzyme A desaturase. Cold-induced up-regulation of gene transcription resulted in a 10-fold increase in desaturase transcript amounts after 48 to 60 hours. However, this increase was preceded by the activation of latent desaturase, probably by a posttranslational mechanism. These two mechanisms may act sequentially to match desaturase expression to the demands imposed by a progressive decrease in temperature.

Cold is a major environmental problem for all living organisms. Poikilothermic animals respond adaptively to chronic cold by a suite of cellular responses that compensate to varying extents for the rate-depressing effects of cooling. The most widespread and consistent response is to increase the unsaturation of membrane phospholipids to offset a cold-induced rigidification of bilayer lipids (*1*, *2*). This "homeoviscous adaptation" is an example of the cell membrane regulation displayed by all cells, yet the enzymes involved have not been clearly identified, and the mechanisms that control their activity are unknown. Cooling of carp liver causes a large increase in the activity of the Δ^9-desaturase (*3*), the enzyme that incorporates the first unsaturation bond into saturated fatty acids (*4*). Here, we investigated the mechanisms underlying this response by measuring amounts of desaturase transcript and protein.

Carp that had been maintained at 30°C for at least 3 months were cooled over 3 days to 10°C and held at 10°C (*5*). At intervals, the carp were killed and liver microsomes were prepared. Figure 1 shows changes in the fatty acid composition of the

P. E. Tiku, A. Y. Gracey, A. I. Macartney, A. R. Cossins, Environmental Physiology Research Group, Department of Environmental and Evolutionary Biology, University of Liverpool, Liverpool L69 3BX, UK.
R. J. Beynon, Department of Applied Biochemistry and Molecular Biology, University of Manchester Institute of Science and Technology, Manchester M60 1QD, UK.

*To whom correspondence should be addressed.

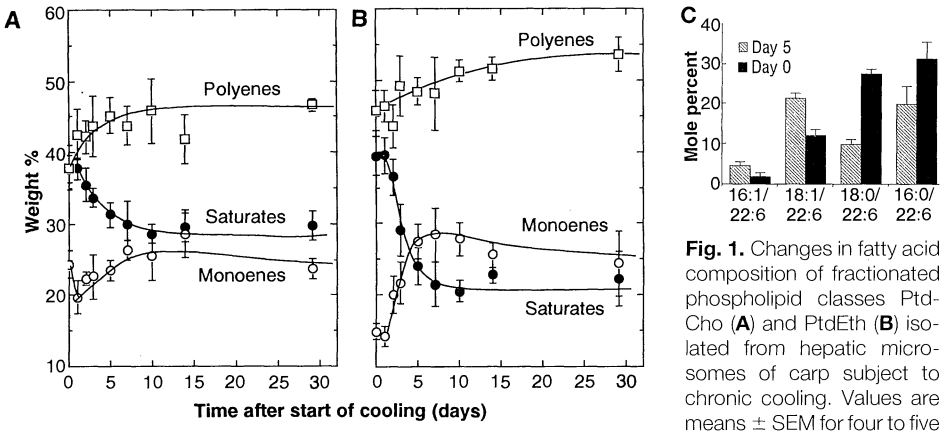

Fig. 1. Changes in fatty acid composition of fractionated phospholipid classes PtdCho (**A**) and PtdEth (**B**) isolated from hepatic microsomes of carp subject to chronic cooling. Values are means ± SEM for four to five individual carp. (**C**) Changes in the distribution of molecular species of PtdEth containing 22:6 between days 0 and 5. The numbers before and after the colon denote the numbers of carbon atoms and double bonds, respectively. Fatty acids occur on phosphoglycerides in pairs, with a saturate or monounsaturate in the *sn-1* position and a polyunsaturate in the *sn-2* position.

two major membrane phosphoglycerides, phosphatidylcholine (PtdCho) and phosphatidylethanolamine (PtdEth). PtdEth showed a large increase in monoenes and smaller increases in polyenes at the expense of saturated fatty acids. These changes became evident 2 days after the initiation of cooling and were complete by day 5. PtdCho showed more complex changes, with polyunsaturates increasing by 24 hours and monoenes decreasing by a corresponding amount. The monoenes subsequently increased at the expense of saturates. The predominant effect was the replacement of saturates by monounsaturates in the *sn-1* position (Fig. 1C), a reaction that is mediated by the Δ^9-desaturase (6).

We cloned the carp Δ^9-desaturase by screening a commercial carp hepatic complementary DNA (cDNA) library with a rat Δ^9-desaturase cDNA under hybridization conditions of moderate stringency (*7*, *8*). This procedure yielded three clones that tested positive in Northern blot analyses of mRNA extracts from cold-exposed carp liver under conditions of very high stringency. All three clones detected a transcript of ~2.7 kb. Clone pcDsL7 had a single open reading frame (ORF) that encoded a polypeptide of 292 amino acid residues (Fig. 2A) and a calculated molecular mass of 33.65 kD. The predicted protein showed a high degree of sequence identity with other published desaturase sequences, including rat liver (55% identity), mouse liver (53% identity), tick (47% identity), and yeast (20% identity). Hydropathy analyses for the carp and rat desaturases (Fig. 2B) revealed considerable similarity in the overall profile, which, when combined with the marked identity of carp, rat, and yeast amino acid sequences and the presence of the fatty acid desaturase 1 (FADs1) consensus site, establishes that pcDsL7 codes for the carp Δ^9-desaturase.

Clone pcDsL7 was used to design an antisense RNA probe for a ribonuclease protection assay (RPA) of desaturase transcript amounts; probes were also prepared for carp 18S rRNA and for carp β-actin (9). All three probes were simultaneously incubated with hepatic RNA extracts (Fig. 3A). The hepatic Δ^9-desaturase transcript amounts varied during chronic cooling relative to 18S ribosomal RNA (rRNA) (Fig.

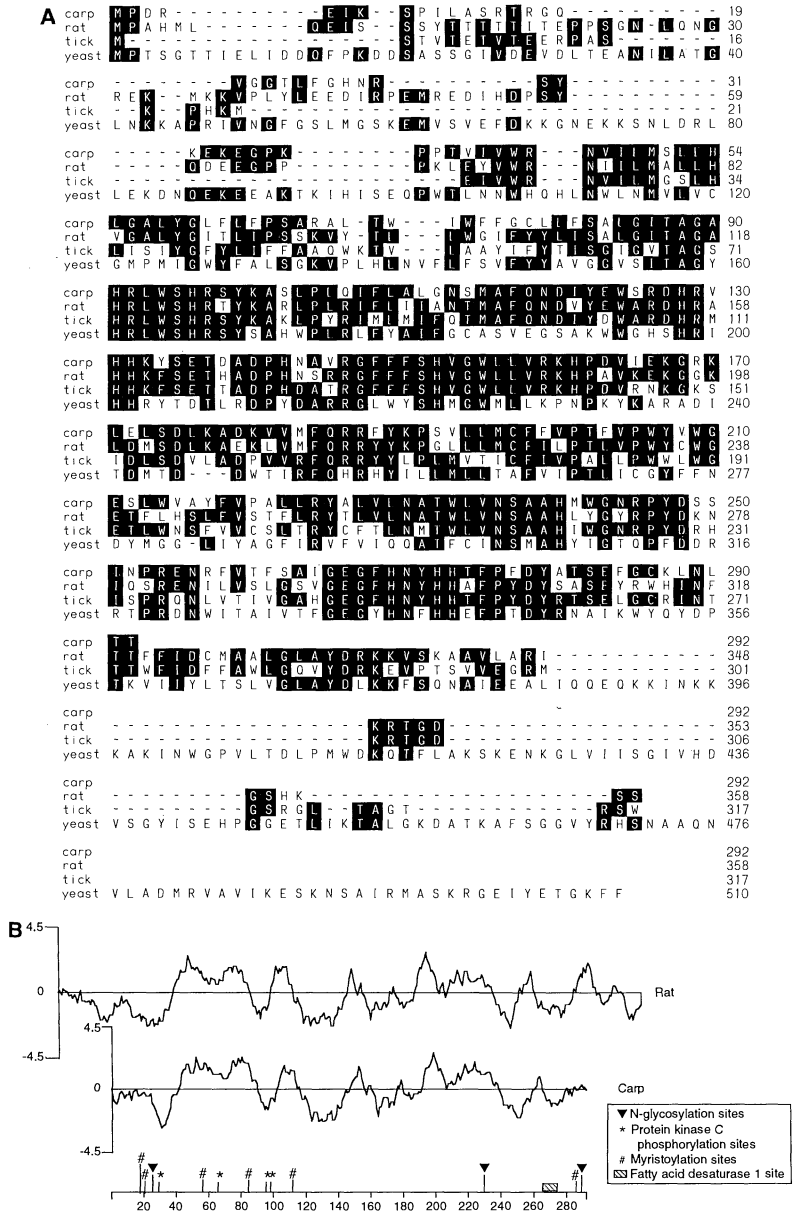

Fig. 2. (**A**) Comparison of the predicted amino acid sequences for Δ^9-desaturases of carp, rat, tick, and yeast. Sequences are in single-letter amino acid codes (*12*). Residues that match the consensus exactly are indicated in reverse type. (**B**) Kyte-Doolittle hydropathy plots for carp and rat Δ^9-desaturases. Each plot was computed with a 12–amino acid window. The bottom panel shows the consensus posttranslational modification sites for carp liver Δ^9-desaturase as identified by a PROSITE library search.

3B) and β-actin mRNA (Fig. 3C). This not only corrects for variations in loading of gels but also reveals the degree to which desaturase transcript amounts exceed those of genes unrelated to the adaptation of lipid composition. In both cases, desaturase transcript amounts were low in warm-acclimated carp and after 24 hours of cooling, but increased greatly in some individuals after 48 hours. Amounts peaked at 3 to 5 days and then quickly subsided to low but measurable amounts for up to 28 days. Thus, although cooling led to a large increase in desaturase transcript amounts, the effect was transient. Steady-state amounts of transcript in cold-acclimated carp were about two to three times those in warm-acclimated carp.

The increase in desaturase transcript amounts might be the result of increased rates of transcription or reduced rates of mRNA degradation or both. We attempted to distinguish between these two possibilities by measuring the rates of desaturase transcript synthesis in isolated nuclei (nuclear run-on assay), a condition that ensures the absence of posttranslational cytoplasmic degradation. Transcript amounts were determined by RPA (Fig. 3D). Nuclei from carp subjected to the cooling regime for 5 days synthesized transcript, whereas those from warm-acclimated carp did not; this finding indicated that desaturase transcription was inactive in warm-acclimated fish but was induced on cooling. Because this effect was observed in nuclei incubated during run-on at both 10° and 30°C, acute cold exposure of isolated nuclei does not in itself activate desaturase transcription, nor does acute warm exposure cause its inhibition. Thus, cold-induced up-regulation of desaturase transcription is mediated by the in vivo thermal history of the nuclei.

Desaturase protein was measured with an antibody raised against rat desaturase. This antibody binds to a carp protein with a molecular mass of ~33 kD (*10*), which agrees with the size predicted from the nucleotide sequence of pcDsL7. Warm-acclimated carp (day 0) had large quantities of immunodetectable desaturase protein relative to the small amount of desaturase activity, although these quantities appeared to increase by day 5 (Fig. 4A). This increase was quantified by densitometric analysis (Fig. 4B); desaturase protein amounts remained constant between days 0 and 3, but increased by ~80% between days 3 and 5. However, Fig. 4C shows that the specific activity of desaturase had already increased on days 2 and 3, before the amounts of desaturase protein had changed. Activity continued to increase between days 3 and 5, corresponding to the increase in desaturase protein. Expressing desaturase specific activity in relation to the amount of desaturase protein gives 3.5 ± 0.5

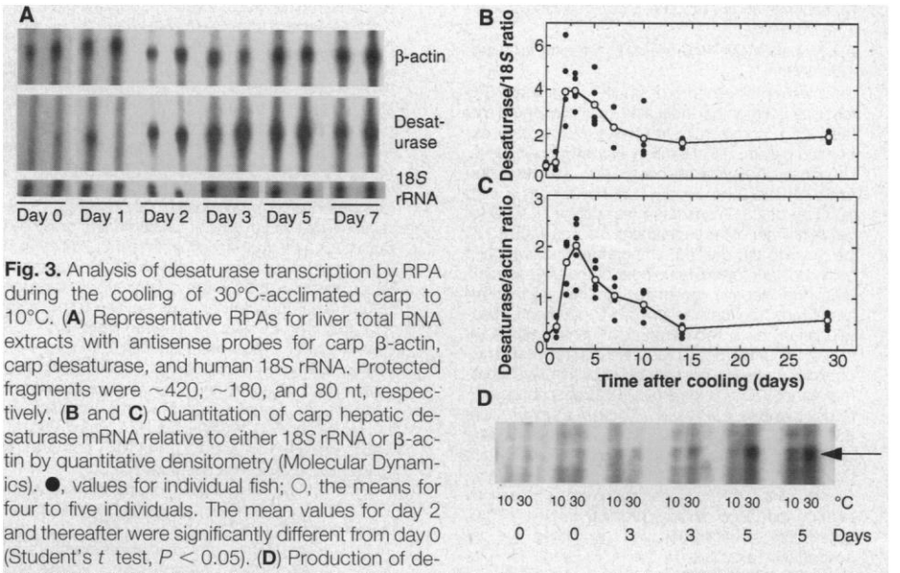

Fig. 3. Analysis of desaturase transcription by RPA during the cooling of 30°C-acclimated carp to 10°C. (**A**) Representative RPAs for liver total RNA extracts with antisense probes for carp β-actin, carp desaturase, and human 18*S* rRNA. Protected fragments were ~420, ~180, and 80 nt, respectively. (**B** and **C**) Quantitation of carp hepatic desaturase mRNA relative to either 18*S* rRNA or β-actin by quantitative densitometry (Molecular Dynamics). ●, values for individual fish; ○, the means for four to five individuals. The mean values for day 2 and thereafter were significantly different from day 0 (Student's *t* test, $P < 0.05$). (**D**) Production of desaturase transcript during nuclear run-on analysis of hepatic nuclei obtained from 30°C-acclimated carp or from day 3 and day 5 cold-acclimated carp. The results were obtained with two fish at each time point. Run-on incubations were performed at 10° or 30°C, as indicated, and transcript amounts were determined by RPA with the antisense desaturase probe.

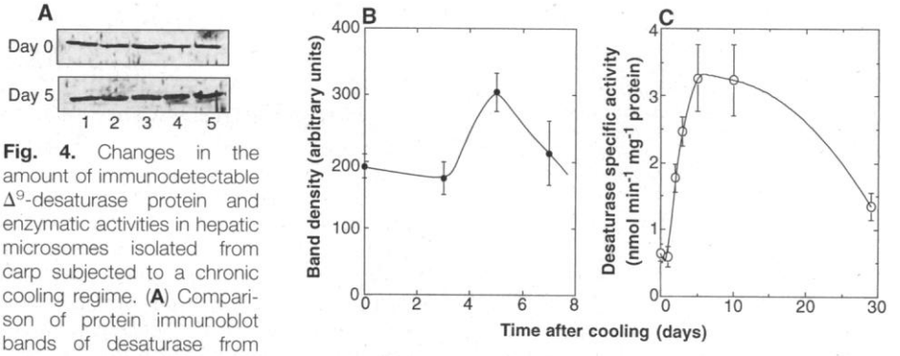

Fig. 4. Changes in the amount of immunodetectable Δ^9-desaturase protein and enzymatic activities in hepatic microsomes isolated from carp subjected to a chronic cooling regime. (**A**) Comparison of protein immunoblot bands of desaturase from 30°C-acclimated carp (day 0) and 5 days after cooling to 10°C. Each band was from a separate carp. (**B**) Changes in amounts of immunodetectable desaturase protein estimated by densitometric analysis. Day 0 and day 3 values were not different (Student's *t* test, $P = 0.53$, $n = 4$ to 6), whereas day 5 values were significantly greater than those for day 0 ($P = 0.011$, $n = 5$ to 6). (**C**) Changes in desaturase specific activity. Methods are described in (*13*).

(arbitrary units, mean ± SEM) for day 0, but 15.1 ± 2.3 and 11.2 ± 2.2 for days 3 and 5, respectively, a three- to fivefold difference.

We suggest that cold-induced Δ^9-desaturase expression arises from two responses. First, a preexisting latent desaturase becomes activated 24 to 48 hours after initiation of cooling. This might include the release of sequestered enzyme or activation by posttranslational modification. Carp desaturase is notable in that it has many consensus sites for phosphorylation, myristoylation, and N-glycosylation (see Fig. 2B). Second, the amounts of desaturase transcript are increased as a result of cold-induced gene transcription, resulting in an increased amount of desaturase protein between days 3 and 5 and a further increase in desaturase activity. Both events correlate in time course and in direction with changes in lipid saturation and membrane lipid order (*11*). The control of desaturase expression is clearly complex and may be related to the extent of cooling: The posttranslational effect may be an early response to moderate cooling, whereas transcriptional up-regulation and increased desaturase protein may require much lower temperatures and consequently a more extensive membrane restructuring. This hierarchy of induction provides a flexible means of matching the magnitude of desaturase expression to the adaptive needs of the tissue.

REFERENCES AND NOTES

1. A. R. Cossins, Ed., *Temperature Adaptation of Biological Membranes* (Portland Press, London, 1994).
2. J. R. Hazel, *Annu. Rev. Physiol.* **57**, 19 (1995).

3. M. Schünke and E. Wodtke, *Biochim. Biophys. Acta* **734**, 70 (1983).
4. A. I. Macartney, B. Maresca, A. R. Cossins, in (*1*), pp. 129–139.
5. Carp were maintained in 2000-liter aquaria at 30°C for at least 3 months under a 12-hour day length and fed with a commercial trout diet (Mainstream expanded pellets; B.P. Nutrition, Northwich, Cheshire, UK). They were gradually cooled over a 3-day period from 30°C to 23°C on day 1, 17°C on day 2, and 10°C on day 3 (*3*) and were maintained at 10°C for the remainder of the experiment. Cooling was at 1°C per hour to the desired temperature and was then held constant for the remainder of the day. At intervals, the hepatic postmitochondrial microsomal membrane fraction was isolated by differential centrifugation and recovered by centrifugation at 100,000*g* for 60 min. Lipids were isolated and phospholipid fractions were separated by thin-layer chromatography and transmethylated as described [A. R. Cossins and C. L. Prosser, *Biochim. Biophys. Acta* **687**, 303 (1982)]. The resulting methyl esters were analyzed by capillary gas chromatography (25 m × 0.25 mm; FFAP, Phase Separations, Queensferry, Clwyd, UK). Molecular species were analyzed by high-performance liquid chromatography (HPLC) separation of dinitrobenzene derivatives as described [H. Takamura, H. Narita, R. Urade, M. Kito, *Lipids* **21**, 356 (1986)].
6. H. G. Enoch, A. Catala, P. Strittmatter, *J. Biol. Chem.* **251**, 5095 (1976).
7. P. Strittmatter, M. A. Thiede, C. S. Hackett, J. Ozols, *J. Biol. Chem.* **263**, 2532 (1988).
8. A commercial carp liver cDNA library (Stratagene) was screened with the Bam HI–Sac I fragment from pDs3-358 (*7*) labeled with [α-^{32}P]deoxycytidine 5′-triphosphate (dCTP) by random priming (Stratagene Prime-It II kit). Hybridization was done in 50% formamide, 5× standard saline citrate (SSC), 5× Denhardt's solution, 1% SDS, and calf thymus DNA (100 μg/ml) at 30°C. Posthybridization washes were done twice for 20 min in 2× SSC and 0.1% SDS at 21°C and 30°C, respectively, and in 0.2× SSC and 0.1% SDS at 30°C. Plasmid pcDsL7 was excised from purified positive lambda plaque CL7 according to manufacturer's (Stratagene) instructions. The full cDNA insert was removed by Kpn I–Sac I digestion and labeled with [α-^{32}P]dCTP as above. RNA was extracted from carp liver [P. Chomzynski and N. Sacchi, *Anal. Biochem.* **162**, 156 (1987)] polyadenylated [poly(A)$^+$] RNA selected and separated by electrophoresis in 1% agarose-formaldehyde followed by capillary transfer to polyvinylidene difluoride (PVDF) membrane [J. Sambrook, E. F. Fritsch, T. Maniatis, *Molecular Cloning: A Laboratory Manual* (Cold Spring Harbor Laboratory Press, Cold Spring Harbor, NY, 1989, vol. 1)]. Blots were hybridized to the full-length cDNA insert from pcDsL7 at 42°C with the same medium as detailed above with highly stringent posthybridization washes according to manufacturer's (Millipore) instructions. The hybridization product was 2.7 kb (P. E. Tiku, data not shown). Unidirectional deletion subclones of pcDsL7 were generated by exonuclease III digestion (Erase-a-base; Promega) and autosequenced (Applied Biosystems model 373A) with universal pUC/M13 primers. The full sequence was confirmed by autosequencing of the anticoding strand as having 2652 bp with an ORF of 879 bp, with a 520-bp 5′ untranslated region (UTR) and a 1253-bp 3′ UTR (GenBank, accession number CCU31864). Translation of this ORF indicated a polypeptide of 292 amino acid residues and a calculated molecular mass of 33.65 kD. For the clustal alignment (Fig. 2B), we used an identity residue weight table and DNAStar Lasergene software. Amino acid sequences were obtained from cDNA sequences from GenBank and EMBL: rat (accession number J02585), tick (U03281), and yeast (J05676).
9. Total RNA (2.5 μg) isolated from carp livers was hybridized at 45°C simultaneously to antisense probes for carp desaturase, carp β-actin, and human 18*S* rRNA (Ambion, Austin, TX). Ribonuclease protection assay was performed with the RPA-II kit from Ambion. Probes were synthesized by in vitro transcription with T7 RNA polymerase (MAXIscript; Ambion) and α-^{32}P uridine 5′-triphosphate. The β-actin template was derived by subcloning the Sac I–Xba I fragment from CA16–Sal I [Z. Liu *et al.*, *DNA Sequence–J. DNA Sequencing and Mapping* **1**, 125 (1990)] into the Promega vector pGEM7Zf(+). The recombinant clone pG7ccactb was digested with Hpa I to generate a template from which a probe of ~700 nucleotides (nt) was synthesized. Unidirectionally deleted pcDsL7 resulted in subclone pcDsL7D*, which had all of the 5′ UTR deleted. This was digested with Xho I and protected with α-phosphorothioate deoxynucleotide triphosphates. Unidirectional deletion of Hind III–digested and protected pcDsL7D* resulted in subclone pcDsL7d4, which was digested with Nae I to give an 830-bp fragment, which was then used as a template for producing the 300-nt desaturase antisense probe. The 109-nt anti–18*S* rRNA probe was synthesized from pT7 18*S* RNA (Ambion). Nuclei were isolated from carp liver, RNA synthesized with unlabeled nucleotide triphosphates [W. F. Marzluff and R. C. C. Huang, in *Transcription and Translation: A Practical Approach*, B. D. Hames and S. J. Higgins, Eds. (IRL Press, Oxford, 1984), pp. 89–130] and 10 μg of RNA analyzed by RPA with the antisense desaturase probe.
10. A. I. Macartney, P. Tiku, A. R. Cossins, in preparation.
11. E. Wodtke and A. R. Cossins, *Biochim. Biophys. Acta* **1064**, 343 (1991).
12. Abbreviations for the amino acid residues are as follows: A, Ala; C, Cys; D, Asp; E, Glu; F, Phe; G, Gly; H, His; I, Ile; K, Lys; L, Leu; M, Met; N, Asn; P, Pro; Q, Gln; R, Arg; S, Ser; T, Thr; V, Val; W, Trp; and Y, Tyr.
13. Equal quantities of microsomal protein were subjected to 12% SDS–polyacrylamide gel electrophoresis, wet-electroblotted onto PVDF membrane, and probed with polyclonal antibody to rat desaturase (*7*). The use of this antibody against a 33-kD carp protein has been described (*10*). In Fig. 4A, the secondary antibody was goat antibody to rat immunoglobulin G conjugated to alkaline phosphatase, and the substrate was 5-bromo-4-chloro-3-indolyl phosphate (BCIP). All bands shown in Fig. 4A were run on the same gel. For the assays shown in Fig. 4B, the chemiluminescent substrate Lumiphos 530 (Boehringer-Mannheim) was used. Exposed x-ray films were analyzed with a Molecular Dynamics (Sunnyvale, CA) laser densitometer, correcting for variations in background and normalizing against a rat desaturase standard for variations between blots in band density. Band density was proportional to protein loading ($r^2 > 0.95$). Δ^9-Desaturase activity was assayed at 30°C by measuring the rate of conversion of palmitoyl-CoA (final concentration, 12.5 μmol/liter) to palmitoleoyl-CoA with trace quantities of ^{14}C-labeled substrate [J. B. Leifkowith, *Biochim. Biophys. Acta* **1044**, 13 (1990)].
14. We thank E. Fodor for HPLC analyses of molecular species; P. Strittmatter for providing the antibody to rat desaturase and the cloned rat cDNA, pDs3-358; P. B. Hackett for the carp β-actin clone CA16–Sal I, and M. Caddick, B. Maresca, and J. Crampton for helpful discussions. Supported by a grant and postgraduate support from the Natural Environmental Research Council (UK).

12 September 1995; accepted 1 December 1995

Identification of a Committed Precursor for the Mast Cell Lineage

Hans-Reimer Rodewald,* Mark Dessing, Ann M. Dvorak, Stephen J. Galli

Mast cells originate from hematopoietic stem cells, but the mast cell–committed precursor has not been identified. In the study presented here, a cell population in murine fetal blood that fulfills the criteria of progenitor mastocytes was identified. It is defined by the phenotype Thy-1^{lo}c-Kit^{hi}, contains cytoplasmic granules, and expresses RNAs encoding mast cell–associated proteases but lacks expression of the high-affinity immunoglobulin E receptor. Thy-1^{lo}c-Kit^{hi} cells generated functionally competent mast cells at high frequencies in vitro but lacked developmental potential for other hematopoietic lineages. When transferred intraperitoneally, this population reconstituted the peritoneal mast cell compartment of genetically mast cell–deficient *W/W*^{v} mice to wild-type levels.

Mature mast cells reside in mucosal and connective tissues where they can act as key mediators in immunoglobulin E (IgE)–dependent allergic reactions. In addition, through the release of cytokines as well as proteases and other mediators, mast cells can participate in a wide array of immunological and inflammatory responses in which they function in the recruitment of leukocytes into sites of inflammation and in the local regulation of vascular or epithelial permeability (*1*). Mast cells originate from hematopoietic stem cells (HSCs) (*2*), and in vitro assays of colony formation indicate that mast cell precursor activity occurs at low frequency in the bone marrow, peripheral blood, and mesenteric lymph nodes of murine rodents (*3*, *4*). It has been proposed that mast cell precursors leave the bone marrow, migrate in the peripheral blood, and invade mucosal and connective tissues where they undergo differentiation into morphologically characteristic mature mast cells. However, a mast cell–committed precursor cell, that is, a cell type distinguished by morphology and developmental potential from a multipotent HSC, has not been purified from bone marrow or blood (*3*, *4*). Here, we report the identification of a cell population purified from murine fetal blood that satisfies the criteria of a mast cell–committed precursor at a stage before tissue

H.-R. Rodewald and M. Dessing, Basel Institute for Immunology, Grenzacherstrasse 487, CH-4005 Basel, Switzerland.
A. M. Dvorak and S. J. Galli, Department of Pathology, Beth Israel Hospital, Harvard Medical School, 330 Brookline Avenue, Boston, MA 02215, USA.

*To whom correspondence should be addressed. E-mail: rodewald@bii.ch